

## Influence of Flap Angle on the Aeroelastic Behavior of Wing-Flap Configuration Using Fully Coupled Structure-Fluid Interaction Model

Dr. Mauwafak A. Tawfik\* , Dr. Mohammed I. Abu-Tabikh   
& Hayder S. Abd Al-Amir\*\*

Received on: 24/11/2010

Accepted on: 7/4/2011

### Abstract

The influence of trailing edge flap angle on the aeroelastic behavior of a vibrating wing-flap configuration is investigated in this work. For this purpose an aeroelastic numerical model with fully coupled structure-fluid interaction is developed. The flow and structural solvers are coupled via successive iterations within each physical time step. The aerodynamic model is based on a hybrid unsteady panel method which is still a good approach to calculate the unsteady loads. While the nonlinear plate equation solved by an assumed mode method is used to represent the structure wing model. The results for a vibrating rectangular wing-flap configuration in low subsonic attached flow are presented, including the effect of flap angle on the unsteady pressure coefficient, time history of lifting coefficient and aeroelastic behavior of the wing. These results clearly show the effect of strong structure-fluid interaction and illustrate the utility of the present model which may be used in the preliminary stage of the wing design.

**Keywords:** Aeroelastic, Assumed modes method, Structure-fluid interaction.

تأثير زاوية القلاب على سلوك المرونة الهوائية لجناح وقلاب باستخدام نموذج مزدوج تام للتداخل بين الهيكل والمائع

### الخلاصة

تناول البحث الحالي اختبار تأثير زاوية القلاب الخلفي على سلوك المرونة الهوائية لجناح طائفة مهتز . تم بناء نموذج عددي يعتمد على مبدأ تداخل مزدوج لمائع مع الهيكل إذ تم تبادل المعلومات بين حلول الجريان غير المستقر والهيكل أثناء كل خطوة زمنية فيزيائية. تم استخدام طريق الأشرطة غير المستقرة لحساب الأحمال الايروديناميكية والتي لازالت تعتبر طريقة جيدة لحساب الأحمال غير المستقرة . في حين تم استخدام معادلة الصفائح اللاخطية كنموذج رياضي لهيكل الجناح . النتائج المستحصلة من هذا البحث لجناح مستطيل الشكل مع قلاب تمت بأخذ تأثير زاوية القلاب على معامل الضغط غير الثبوتي والتصرف الزمني لمعامل الرفع و سلوك المرونة الهوائية للجناح. أظهرت النتائج تأثير قوي للتداخل بين حركة المائع و الانحرافات الحاصلة والتي يمكن الاستفادة منها في مراحل التصميم الأولية للأجنحة.

\* Machines & Equipments Engineering Department, University of Technology/ Baghdad

\*\* Institute of Technology/Baghdad

**Nomenclature**

$a$	= semi span of the wing	m	$v$	= velocity component in y-direction	m/s
$b$	= chord of the wing	m	$V_\infty$	= air velocity	m/s
$C_L$	= lift coefficient	-	$V_{FR}$	= induced velocity due to unsteady motion of wing	m/s
$C_P$	= pressure coefficient	-	$w$	= plate displacement in z-direction	m
$E$	= modules of elasticity	Pa	$\alpha$	= angle of attack	rad
$h$	= plate thickness	m	$\alpha_{eff}$	= effective angle of attack	rad
$k_{ij}$	= stiffness element	N/m	$\Gamma$	= circulation	m <sup>2</sup> /s
$L$	= length of panel	m	$\gamma$	= vorticity strength	m/s
$m$	= mass per unit area	kg/m <sup>2</sup>	$\gamma_{xy}$	= shear strain	-
$m_{ij}$	= mass element	kg	$\Delta P$	= pressure difference	Pa
$\vec{n}$	= normal unit vector	-	$\Delta t$	= time step	sec.
$Q_i$	= generalized force	N	$\delta$	= node displacement	m
$q_i$	= generalized coordinate	m	$\epsilon_x$	= normal strain in x-direction	-
$q_\infty$	= dynamic pressure	Pa	$\epsilon_y$	= normal strain in y-direction	-
$s$	= distance along the panel	m	$\nu$	= Poisson's ratio	-
$u$	= velocity component in x-direction	m/s	$\phi$	= velocity potential	m <sup>2</sup> /s
$u_s$	= deformation of mid surface in x-direction	m	$\psi_i$	= coordinate function	-
$v_s$	= deformation of mid surface in y-direction	m			

**1-Introduction**

The development of aeroelastic numerical models for utilization in the preliminary design stage of wing structures has become very important and received special attention in recent years. To study aeroelasticity phenomena numerically, the fluid

(aerodynamics) and structure (wing) mathematical models must be taken into account. The fluid and structure governing equations are coupled by exchanging the aerodynamic forces and structure displacement between them.

This exchanging must be achieved simultaneously during the motion process.

Many models of aerodynamics and structure are suggested by researchers. The typical airfoil rigid section and the unsteady lift force model that developed by Theodorsen [1] is used to predict the flutter speed and study the dynamic responses of the wing by many researchers. The beam theory is used so many to describe the wing structure [2,3]. Rakesh, et al. [4], and Gordnier and Visbal [5] analyzed a wing by assuming that it behaves as a plate. Rakesh, et al. [4] state that this assumption is very reasonable as long as the wing has a small thickness to chord ratio.

The aerodynamic loads can be evaluated in several ways. For low subsonic inviscid incompressible flow, the potential-based method such as the panel [6] or vortex lattice one can be used [7,8]. For high supersonic and hypersonic flows, the piston theory aerodynamic may be used [9]. The aerodynamic analysis by solving the full Navier-Stokes equations with (CFD) tools is powerful approach and not limited by certain conditions [10]. However, the using of three dimensional Navier-Stokes aerodynamic models with fully coupled is very hard task when compared with other approaches due to the perplexing physical phenomena and the large amount of computation work. Gordnier and Visbal [5] used unsteady compressible three-dimensional Euler equation to model the aerodynamics coupled with a nonlinear finite element plate model (delta wing). The primary vortical flow features of interest for the

sharp-edged delta wing were simulated. Benini, et al. [7] used vortex lattice method to predict the unsteady aerodynamic loads, the aeroelastic responses of the wing model were found for different airspeeds. Cattarius [8] solved the aeroelastic equation of motion iteratively in time domain. The two-entity numerical code comprised of ABAQUS/Standard and the unsteady-vortex-lattice method was used. Chen and Zha [10] presented a numerical methodology coupling Navier-Stokes equations and plate as structural model (solved by finite element solver) for predicting 3-D transonic wing. The pressure coefficients on the ONERA M6 wing surface at different cross sections were calculated. Abu-Tabikh [11] determined the unsteady aerodynamic load on rectangular wing undergoes assumed harmonic motion in pitch and heaving direction. The vortex panel method was used without structural modeling.

In the present work, the interest is focused on the effect of control surface angle, namely, the trailing edge flap angle on the aeroelastic behavior of a vibrating rectangular wing-flap configuration in low subsonic attached flow. The flow and structural solvers are fully coupled via successive iterations within each physical time step. A hybrid panel-discrete vortex unsteady method combined with the numerical lifting line method is used to describe the aerodynamic model. While the nonlinear plate equation solved by an assumed mode method is used to represent the structure wing model.

## 2-The Aerodynamic Model

An unsteady panel-discrete vortex method using MATLAB computer

program is devised to estimate the unsteady aerodynamic forces acting on vibrating wing-flap configuration, figure (1). In this approach the airfoil section surface is divided into a number of panels. Each panel has vorticity strength  $(\gamma_i(s))$  which change linearly along panel as given in the following equation:

$$\gamma(s_j) = \gamma_j + \frac{s_j}{L_j}(\gamma_{j+1} - \gamma_j) \quad \dots(1)$$

The wing has unsteady motion (eg. heaving motion), wake vortices will be created behind the wing as shown in figure (1); therefore; the velocity components at each mid point of panel are

$$u_{pi} = V_\infty \cos \alpha + \sum_{j=1}^N u_{vij} + \sum_{k=1}^{NV} u_{vik} + V_{FRix}$$

$$v_{pi} = V_\infty \sin \alpha + \sum_{j=1}^N v_{vij} + \sum_{k=1}^{NV} v_{vik} + V_{FRiy} \quad \dots(2)$$

In heaving motion the induced velocity  $V_{FRix} = 0$  and  $V_{FRiy}$  may be approximated by [11]

$$V_{FRiy} = \frac{\delta_{im} - \delta_{im-1}}{\Delta t} \quad \dots(3)$$

where  $\delta_i$  is the displacement of each mid point of panel at each time step comes from vibrated plate (wing).

By using the flow tangency condition (4) , Kutta condition Eq(5) and condition of constant circulation around airfoil Eq (6)

$$\vec{V} \cdot \vec{n} = 0 \quad \dots(4)$$

$$\gamma_1 = \gamma_{N+1} = 0 \quad \dots(5)$$

$$\Gamma_m + \sum_{k=1}^{NV} \Gamma_{vk} = 0 \quad \dots(6)$$

where

$$\Gamma_m = \sum_{j=1}^N L_j [(\gamma_j)_m + (\gamma_{j+1})_m] \quad \dots(7)$$

This leads to the set of linear algebraic equations with unknowns  $\gamma_j$  and  $\Gamma_k$ .

These equations are solved by using Gauss elimination with partial pivoting technique to find  $\gamma_i$  and  $\Gamma_k$  [11]. Then the unsteady pressure coefficient can be obtained from the unsteady Bernoulli's equation [11]

$$Cp_i = 1 - \frac{\gamma_i^2}{V_\infty^2} - \frac{2}{V_\infty^2} \left( \frac{\phi_m - \phi_{m-1}}{\Delta t} \right)_i \quad \dots(8)$$

At time  $t_m$  equation (8) can be used to calculate the pressure coefficient around the section, after integration  $C_L$  values may be obtained at that instantaneous time. Equation (8) has been reused at each step time interval to obtain the time history of  $C_L$ .

To extend the 2-D aerodynamics solution to 3-D, the effective angle of attack at each section along the span must be taken into consideration. The numerical solution for the lifting line theory developed by Anderson, et al [12] is used to determine the angle at each section. Then the unsteady effective angle may be calculated from Eq (9) [6]

$$\alpha_{eff} = \text{angle of attack at each section} + \tan^{-1} \frac{\text{heaving velocity}}{\text{flow velocity}} \quad \dots(9)$$

In this analysis the semi span wing is divided into 20 sections and each section is divided into 140 panels.

**3-Structural Model of a 3D Wing**

The behavior of wing structure during vibration can be treated by using one of the following wing geometry; beam[2,3], walled thin beam[17], and plate[4,5,7,10]. At the present the wing is treated as rectangular flat plate [18]. The governing structural equation that represents the wing is nonlinear plate equation. The source of the nonlinearity comes from assuming large plate deflections [5]. In this assumption the total strains in the layer of the plate parallel to and at distance z from the middle surface can be written as

$$\epsilon_x = \frac{\partial u_s}{\partial x} + \frac{1}{2} \left(\frac{\partial w}{\partial x}\right)^2 - z \frac{\partial^2 w}{\partial x^2} = \frac{1}{2} w_x^2 - z w_{xx}$$

$$\epsilon_y = \frac{\partial v_s}{\partial y} + \frac{1}{2} \left(\frac{\partial w}{\partial y}\right)^2 - z \frac{\partial^2 w}{\partial y^2} = \frac{1}{2} w_y^2 - z w_{yy}$$

$$\epsilon_{xy} = \frac{\partial u_s}{\partial y} + \frac{\partial v_s}{\partial x} + \frac{\partial w}{\partial x} \frac{\partial w}{\partial y} - 2z \frac{\partial^2 w}{\partial x \partial y} = w_x w_y - 2z w_{xy}$$

....(10)

The  $u_s$  and  $v_s$  are uncoupled with  $w$ , this leads to delete the  $u_s$  and  $v_s$  from the plate equations [13].

The strain energy of plate is

$$U = \frac{1}{2} \frac{E}{1-\nu^2} \iint_A \int_{-h/2}^{h/2} ((\epsilon_x^2 + 2\nu\epsilon_x\epsilon_y + \epsilon_y^2) + \frac{(1-\nu)}{2} \gamma_{xy}^2) dz dA$$

....(11)

where

$$\epsilon_x^2 = \left[\frac{1}{2} w_x^2 - z w_{xx}\right]^2 = \frac{1}{4} w_x^4 - z w_x^2 w_{xx} + z^2 w_{xx}^2$$

$$\epsilon_y^2 = \left[\frac{1}{2} w_y^2 - z w_{yy}\right]^2 = \frac{1}{4} w_y^4 - z w_y^2 w_{yy} + z^2 w_{yy}^2$$

$$\gamma_{xy}^2 = [w_x w_y - 2z w_{xy}]^2 = w_x^2 w_y^2 - 4z w_x w_y w_{xy} + 4z^2 w_{xy}^2$$

$$\epsilon_x \epsilon_y = \left[\frac{1}{2} w_x^2 - z w_{xx}\right] \left[\frac{1}{2} w_y^2 - z w_{yy}\right] = \frac{1}{4} w_x^2 w_y^2 - z w_x^2 w_{yy} - \frac{1}{2} z w_{xx} w_y^2 + z^2 w_{xx} w_{yy}$$

....(12)

Substituting Eqs (12) into Eq (11) and integrating to z, yield

$$U = \frac{1}{2} \frac{Eh^3}{1-\nu^2} \iint_A ((\nabla^2 w)^2 + 2(1-\nu)[(w_{xy})^2 - w_{xx} w_{yy}]) dA$$

+ additional terms

Where

$$\text{additional terms} = \frac{1}{2} \frac{E}{1-\nu^2} \iint_A \left[\frac{h}{4} w_x^4 + \frac{h}{4} w_y^4 + 2\nu \left[\frac{h}{4} w_x^2 w_y^2\right] + \frac{1-\nu}{2} [h w_x^2 w_y^2]\right] dA$$

....(13)

The plate kinetic energy is

$$T = \frac{1}{2} \iint_A m \dot{w}^2 dx dy$$

....(14)

The assumed –mode method is used in the derivation of the equations of motion for the plate. This method depends on assuming suitable solution to the displacements of the problem. In plate problem the displacements are assumed to be of the form

$$w(x, y, t) = \psi_1(x, y)q_1(t) + \psi_2(x, y)q_2(t) + \psi_3(x, y)q_3(t) + \dots + \psi_i(x, y)q_i(t)$$

....(15)

where  $q_i(t)$  generalized coordinates, and  $\psi_i(x, y) = X_m(x)Y_n(y)$  are the admissible beam functions.  $X_m(x)$  satisfy

clamped-free boundary conditions and  $Y_n(y)$  free-free conditions, which are defined as follows [14]:

$$X_m(x) = \mu_m \left( \cosh \alpha_m \frac{x}{a} - \cos \alpha_m \frac{x}{a} \right) - \nu_m \left( \sinh \alpha_m \frac{x}{a} - \sin \alpha_m \frac{x}{a} \right)$$

$$\mu_m = \frac{\cosh \alpha_m + \cos \alpha_m}{\sinh \alpha_m \sin \alpha_m}, \quad \dots 16$$

$$\nu_m = \frac{\sinh \alpha_m - \sin \alpha_m}{\sinh \alpha_m \sin \alpha_m}$$

where  $\alpha_m$  are the roots of  $\cosh \alpha_m \cos \alpha_m = -1$   
 $\alpha_1 = 1.875, \alpha_2 = 4.694, \alpha_3 = 7.854, \dots$

$$Y_1(y) = 1, \quad Y_2(y) = \sqrt{3} \left( 2 \frac{y}{b} - 1 \right)$$

$$Y_n(y) = \kappa_n \left( \cosh \beta_n \frac{y}{b} + \cos \beta_n \frac{y}{b} \right) - \lambda_n \left( \sinh \beta_n \frac{y}{b} + \sin \beta_n \frac{y}{b} \right)$$

$$\kappa_n = \frac{\cosh \beta_n - \cos \beta_n}{\sinh \beta_n \sin \beta_n}, \quad \dots 17$$

$$\lambda_n = \frac{\sinh \beta_n + \sin \beta_n}{\sinh \beta_n \sin \beta_n}$$

where  $\beta_n$  are the roots of  $\cosh \beta_n \cos \beta_n = 1$

In this analysis, the displacements are assumed as

$$w(x, y, t) = \psi_1(x, y)q_1(t) + \psi_2(x, y)q_2(t) \quad \dots 18$$

where

$$\psi_1(x, y) = X_1Y_1, \quad \psi_2(x, y) = X_1Y_2$$

Substituting Eqs(18) into Eqs (13&14) and applying Lagrange's equation the

following two differential equations of plate motion are obtained

$$m_{11} \ddot{q}_1 + k_{11}q_1 + k_{12}q_2 + Aq_1^3 + Bq_1^2q_2 + Cq_1q_2^2 + Dq_2^3 + EEq_2^2 = Q_1$$

$$m_{22} \ddot{q}_2 + k_{21}q_1 + k_{22}q_2 + Fq_1^3 + Gq_1^2q_2 + Hq_1q_2^2 + Iq_2^3 + Jq_2q_1^2 = Q_2$$

....(19)

where

$$Q_1 = \iint_A p(x, y, t) X_1 Y_1 dx dy$$

$$Q_2 = \iint_A p(x, y, t) X_1 Y_2 dx dy \quad \dots(20)$$

The constants

$$m_{ij}, k_{ij}, A, B, C, D, EE, F, G, H, I, J$$

are defined in the Appendix (A).

#### 4-Fully Coupled Fluid-Structural Interaction Procedure

Structural systems are very often subjected to transient excitation. A transient excitation is a highly dynamic time-dependent force exerted on structure. The solution starts by assuming that the wing is disturb by initial displacement[18], it is common simulation may be used to simulate the start of vibration due to external source such gust wind or air-trap. The nodes on the plate are displaced by means of the initial generalized coordinates. Then Eqs (19) are solved using Runge-Kutta method to obtain generalized coordinates.

The wing in the aerodynamics model is divided into 140 panels and 20 sections in semi span. The upper and lower nodes in aerodynamics model take their deflections from corresponded

node in structural model (plate). Implementation of Eq (18) the displacement of plate at each node and at each section is determined. These displacements are fed to aerodynamics model (panel method). Solving the panel method gives pressure difference at each node and at each time step (one iteration). Finally these pressure differences are fed to structural model (plate) Eq (19) as a part of the generalized forces  $Q_1, Q_2$ . To use these pressure differences to find generalized forces  $Q_1, Q_2$  ( Eq(20)), the pressure differences must be found as a mathematical function of the independent variable  $x$  &  $y$  of nodes plate at each time step. This can be achieved by using curve fitting between pressure differences and  $x, y$  coordinates of nodes at each time step. The form of the fitting equation is

$$\begin{aligned} \Delta P(x,y) = & P_1 + P_2x + P_3y + P_4x^2 + P_5xy + P_6y^2 + P_7x^3 + P_8x^2y \\ & + P_9xy^2 + P_{10}y^3 + P_{11}x^4 + P_{12}x^3y + P_{13}x^2y^2 + P_{14}xy^3 + P_{15}x^5 \\ & + P_{16}x^4y + P_{17}x^3y^2 + P_{18}x^2y^3 + P_{19}xy^4 + P_{20}y^5 \\ & \dots \quad (21) \end{aligned}$$

where  $P_i$  are constants and calculated at each iteration. The procedure is illustrated in the flow chart given in Fig (2)

The choice of the value of time step ( $\Delta t$ ) is very important to avoid instability of the solution problem .So in this work the time step ( $\Delta t$ ) is 0.0005 second as taken by the work of Chen and Zha [10]. The dimensions and material properties of the plate that are used in this paper are shown in table (1)

### 5-Results and Discussion

The present model is applied to a vibrating wing-flap configuration. The wing is rectangular of NACA 0012 section with  $0.18chord$  plain flap .The wing is subjected to low subsonic flow of 30 m/sec. The geometric angle of attack is  $3 \text{ deg}$ . (i.e. attached flow regime).

To validate the structure model used in the present study, the natural frequencies of the plate wing are calculated by using the assumed mode method and compared with Gorman results [15] and Liang, et al [16]. This was done for linear system with first five natural frequencies as shown in table (2). The present method gives an adequate prediction of the natural frequencies compared with published results.

The effect of flap angle on the surface pressure distribution near the root and at tip is shown in figure (3).The general trend of the pressure curves at different times is typical for attached flow case. A suction peak is indicated on the upper surface at the wing-flap joint. This suction peak is increased with flap angle. It can be seen that the large variation in pressure distribution with time is occurred at the wing tip, where as stable distribution of pressure is indicated near the wing root.

Figure (4), illustrates the effect of flap angle on the lift distribution along the semi-span at different times. The average value of lift is increased with increasing of the flap angle. The values of lift coefficient fluctuated from positive to negative during the oscillatory motion of the wing. However, as the flap angle is increased, favorable behavior of lift coefficient is

observed (almost all values of  $C_L$  have positive sing during the oscillatory motion). This behavior is very clear at wing tip due to high amplitude of oscillation.

Figure (5) shows the time dependent behavior of lift coefficient  $C_L$  at different flap angles. With increasing the flap angles, a circulatory loading is generated on the wing due to unsteady motion. This load will be build up quickly and tends asymptotically to a mean value. This behavior is clear at sections near the wing root where the effective angle of attack at sections near the root is larger than that near the tip [12].

The pressure differences ( $\Delta P$ ) on the wing surface at different flap angles and times are shown in figure (6). The peak in the pressure differences at wing flap joint is proportional with the increasing of flap angle.

The effect of amplitude of oscillation is pronounced on the aeroelasticity responses of the wing as shown in figure (7). It is obvious from figure (7), the flap angle has a great effect on the response and mode of vibration for the wing. Also it shows that as the flap angle increases at each specific time step, the system tends to vibrates in higher mode of vibration. This behavior in turn affects the aerodynamic pressure differences distribution and other aerodynamic properties on the wing surface.

Figure (8) shows a typical time history of the deflection at three nodes (leading, middle and trailing) and at different sections along the semi span of the wing for  $\alpha_g = 3 \text{ deg}$ , zero degree flap angle and eight degree flap angle. The effect of the flap angle on the nodes

deflection is very clear. The deflection of the nodes at different sections increase with increasing in flap angle. Also the variation of the deflection with respect to time is increasing and that explain why the fluctuation in lift coefficient in figure (5) varies with increasing of flap angle. The reason is, the fluctuation in lift coefficient depends on the induced velocity due to unsteady motion of wing. The induced velocity depends on variation of the deflection during time step ( $\Delta t = 0.0005 \text{ sec}$ ) Eq (3). Another result can be deduced from Figure (8), the wing deflections can be viewed as a mean deflection with a fluctuation peak to peak about the mean value with time.

Figure (9) shows the lift coefficient as a function of generalized coordinates  $q_1$  and  $q_2$ . Hysteresis is clearly evident. The hysteresis loops are traversed in anticlockwise direction. A qualitative comparison between the present results and the results of Abu-Tabikh [11] is made. Acceptable agreement is obtained, since in Abu-Tabikh work [11] the unsteady motion of the wing was a result of an assumed harmonic function independent on the aeroelastic response (i.e. uncoupled solution). While in the present work the unsteady motion of the wing is generated from the aeroelastic response (i.e. coupled solution).

## 6-Conclusions

The influence of flap angle on aerodynamic coefficients and aeroelastic response of a vibrating rectangular wing-flap configuration is investigated in this work. For this purpose an aeroelastic numerical model with fully coupled fluid-structure interaction has been developed. The

principal conclusions may be summarized as follows:

- A peak in the pressure difference is indicated on the wing surface at the wing-flap joint. This peak is proportional with the increasing of flap angle.

- The flap angle has considerable effect on the time dependent behavior of lift coefficient. The variation of lift coefficient from positive to negative during the oscillatory motion is very clear at wing tip where the lift exhibits more of fluctuations. Favorable behavior of lift coefficient is observed when the flap angle is increased.

- The effect of flap angle is pronounced on the aeroelasticity behavior of the wing. This may change the aerodynamic coefficients of the wing. The fluctuation in lift coefficient depends on variation of the deflection of each node.

- The hysteresis loops of unsteady lift coefficient clearly show the effect of strong structure-fluid interaction and the resulting aeroelastic response of the vibrating wing.

- The results presented in this work illustrate the utility of the present model, which may be used in the preliminary stage of wing design or may be used as a part of more sophisticated studies like neural controller on flutter by using wing control surfaces.

#### References

- [1] Theodorsen, T. "General theory of aerodynamic instability and the mechanism of flutter", NACA Report , No.496,1939.
- [2] Moosavi, M.R., Oskouei, M.R. and Kheli, A. " Flutter of subsonic wing", Thin-Walled Structures ,Vol.43, 2005,pp 617–627.
- [3] Abbas, L. K., Chen, Q. and Milanese, A. " Non-linear aeroelastic investigations of store(s)-induced limit cycle oscillations", Journal of Aerospace Engineering , Vol. 222 Part G, 2008.
- [4] Rakesh, K. and Liu, Y. "Static and Vibration Analyses of General Wing Structures Using Equivalent Plate Models", AIAA, 2000.
- [5] Gordnier, R.E. and Visbal, M.R. " Computation of the aeroelastic response of a flexible delta wing at high angle of attack", Journal of Fluids and Structures ,Vol. 19,2004,pp.785-800.
- [6] Mantia , M. L. and Dabnichki, P. " Unsteady panel method for flapping foil", Engineering Analysis with Boundary Elements, Vol.33, 2009 , pp.572-580.
- [7] Benini, G.R., Belo, E.M. and Marques, F.D. "Numerical model for simulation of Fixed wings aeroelastic response", J. of the Braz. Soc. of mech. Sci. Eng., Vol. XXVI, No.2/129, 2004.
- [8] Cattarius, J. " Numerical wing/store interaction analysis of a parametric F16 wing", Ph.D thesis , Faculty of the Virginia Polytechnic Institute and State University ,1999.
- [9] Abbas, L. K., Chen, Q. and Valentinem, D. "Numerical studies of a non-linear aeroelastic system with plunging and pitching freeplays in supersonic/hypersonic regimes", Aerospace Science and Technology, Vol.11, 2007,pp. 405-418.
- [10] Chen, X. and Zha, G. "Numerical Simulation of 3-D Wing Flutter with Fully Coupled Fluid- Structural Interaction", Computers & Fluids, Vol.36 , 2007,pp.856-867.

[11] Abu-Tabikh, M.I. " Modeling of Steady and Unsteady Turbulent Boundary Layer Separation Using Vortex Hybrid Method ", Ph.D thesis, Department of Mechanical Engineering, U.O.T, Baghdad, 1997.

[12] Anderson, Jr., J.D. , Corda, S. and Van Wie , D.M. "Numerical lifting Line theory Applied to Drooped Leading -Edge Wing Below and Above stall", Journal of Aircraft , Vol. 17 ,No.12, 1980, pp.898-904.

" , Journal of Sound and Vibration, Vol.

[13] Irving H. S., Energy and Finite Element Methods in Structural Mechanics, McGraw-Hill Book Company, 1985.

[14] Chiba, M. and Sugimoto, T. "Vibration characteristics of a cantilever plate with attached spring-mass system 260, 2003, pp. 237-263.

[15] Gorman, D. J. Free Vibration Analysis of Rectangular Plates, Elsevier North Halland, Inc, 1982.

[16] Liang, C. C., Liao, C.C. and Tai, Y. S. "The Free Vibration Analysis of Submerged Cantilever Plates", Ocean Engineering , Vol. 28, 2001, pp. 1225-1245.

[17] Qin, Z. "Vibration and Aeroelasticity of Advanced Aircraft Wings Modeled as Thin-Walled Beams - Dynamics, Stability and Control", Ph.D. thesis, The Faculty of the Virginia Polytechnic Institute and State University, 2001.

[18] Ke, S., Zhigang, W. and Chao, Y. "Analysis and Flexible Structural Modeling for Oscillating Wing Utilizing Aeroelasticity", Chinese Journal of Aeronautics. Vol. 21, 2008, pp.402-410.

**Appendix (A)**

The constants of the plate equations

$$m_{ij} = \int_A m \psi_i \psi_j dA$$

$$k_{ij} = \sum_{q=1}^2 \sum_{p=1}^2 a_{ijpq} + 2(1-\nu)(b_{ij} - a_{ij12})$$

[13]

$$a_{ijpq} = \frac{Eh^3}{12(1-\nu^2)} \iint_A \frac{\partial^2 \psi_i}{\partial x_p^2} \frac{\partial^2 \psi_j}{\partial x_q^2} dA \quad b_{ij} = \frac{Eh^3}{12(1-\nu^2)} \iint_A \frac{\partial^2 \psi_i}{\partial x_1 \partial x_2} \frac{\partial^2 \psi_j}{\partial x_1 \partial x_2} dA$$

$$A = \frac{1}{2(1-\nu^2)} \int_A (h\psi_{1x}^4 + h\psi_{1y}^4 + 2h\psi_{1x}^2\psi_{1y}^2 + 2(1-\nu)h\psi_{1x}^2\psi_{1y}^2) dA$$

$$B = \frac{1}{2(1-\nu^2)} \int_A (3h\psi_{1x}^3\psi_{2x} + 3h\psi_{1y}^3\psi_{2x} + h(3\psi_{1x}^2\psi_{1y}\psi_{2y} + 3\psi_{1x}\psi_{2x}\psi_{1y}^2 + \psi_{2x}^2\psi_{1y}^2) + \dots$$

$$(1-\nu)h(3\psi_{1x}^2\psi_{1y}\psi_{2y} + 3\psi_{1x}\psi_{2x}\psi_{1y}^2 + \psi_{2x}^2\psi_{1y}^2)) dA$$

$$C = \frac{1}{2(1-\nu^2)} \int_A (3h\psi_{1x}^2\psi_{2x}^2 + 3h\psi_{1y}^2\psi_{2y}^2 + h(\psi_{1x}^2\psi_{2y}^2 + 4\psi_{1x}\psi_{2x}\psi_{1y}\psi_{2y} + \psi_{2x}^2\psi_{1y}^2) + \dots$$

$$(1-\nu)h(\psi_{1x}^2\psi_{2y}^2 + 4\psi_{2x}\psi_{1x}\psi_{2y}\psi_{1y} + \psi_{2x}^2\psi_{1y}^2)) dA$$

$$D = \frac{1}{2(1-\nu^2)} \int_A (h\psi_{1x}\psi_{2x}^3 + h\psi_{1y}\psi_{2x}^3 + \nu h\psi_{2x}^2\psi_{1y}\psi_{2y} +$$

$$(1-\nu)h\psi_{2x}^2\psi_{1y}\psi_{2y}) dA$$

$$EE = \frac{1}{2(1-\nu^2)} \int_A (\nu h\psi_{1x}\psi_{2x}\psi_{2y} + (1-\nu)h\psi_{1x}\psi_{2x}\psi_{2y}) dA$$

$$F = \frac{1}{2(1-\nu^2)} \int_A (h\psi_{1x}^3\psi_{2x} + h\psi_{1y}^3\psi_{2y} + \nu h\psi_{1x}^2\psi_{1y}\psi_{2y} + h\psi_{1x}\psi_{2x}\psi_{1y}^2 +$$

\dots

$$(1-\nu)h(\psi_{1x}^2\psi_{1y}\psi_{2y} + \psi_{1x}\psi_{2x}\psi_{1y}^2)) dA$$

$$G = \frac{1}{2} \frac{E}{1-\nu^2} \int_A (3h\psi_{1x}^2\psi_{2x}^2 + 3h\psi_{1y}^2\psi_{2y}^2 + \nu h\psi_{1x}^2\psi_{2y}^2) \frac{1}{2} \frac{E}{1-\nu^2} \int_A (2\nu h\psi_{1x}\psi_{2x}\psi_{2y} + 2(\nu-1)h\psi_{1x}\psi_{2x}\psi_{2y}) dA$$

$$+ 2\nu h(4\psi_{2x}\psi_{1x}\psi_{2y}\psi_{1y} + \psi_{2x}^2\psi_{1y}^2) + \dots$$

$$(1-\nu)h(\psi_{1x}^2\psi_{2y}^2 + 4\psi_{2x}\psi_{1x}\psi_{2y}\psi_{1y} + \psi_{2x}^2\psi_{1y}^2) dA$$

$$H = \frac{1}{2} \frac{E}{1-\nu^2} \int_A (3h\psi_{1x}\psi_{2x}^3 + 3h\psi_{1y}\psi_{2y}^3 + 3\nu h\psi_{2x}^2\psi_{1y}\psi_{2y} + 3(\nu-1)h\psi_{2x}^2\psi_{1y}\psi_{2y}) dA$$

$$I = \frac{1}{2} \frac{E}{1-\nu^2} \int_A (h\psi_{2x}^4 + h\psi_{2y}^4 + 2\nu h + 2(\nu-1)h\psi_{2x}^2\psi_{2y}^2) dA$$

**Table (1) The plate properties**

<i>a</i>	1.5m
<i>b</i>	0.75m
<i>h</i>	0.025m
<i>ν</i>	0.3
<i>E</i>	69×10 <sup>9</sup> Pa
<i>ρ</i>	2768.6 kg/m <sup>3</sup>

**Table (2) first five eigen values for cantilever plate**

Mode	Assumed mode method (present work)	Gorman [15]	Liang, et al [16]
1	3.53281	3.487	3.5
2	8.6230	10.03	8.2
3	23.565	21.78	23
4	27.432	31.07	-
5	32.145	33.88	-

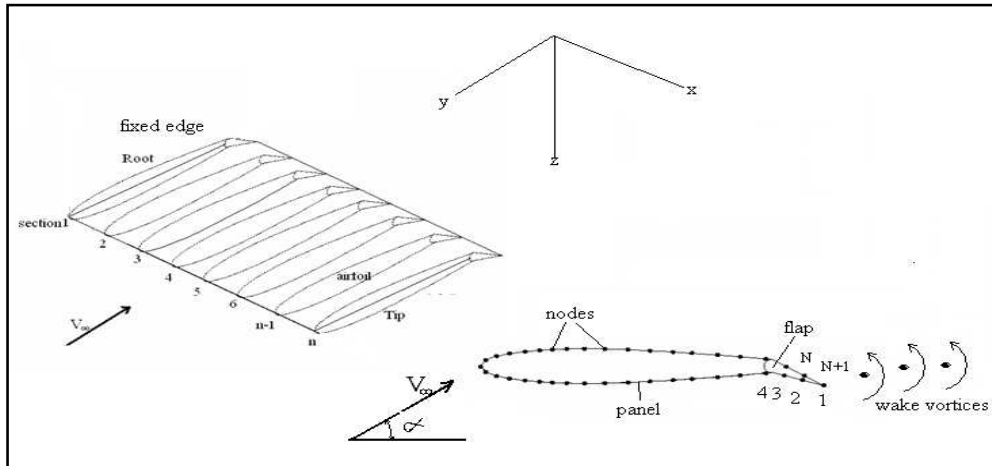
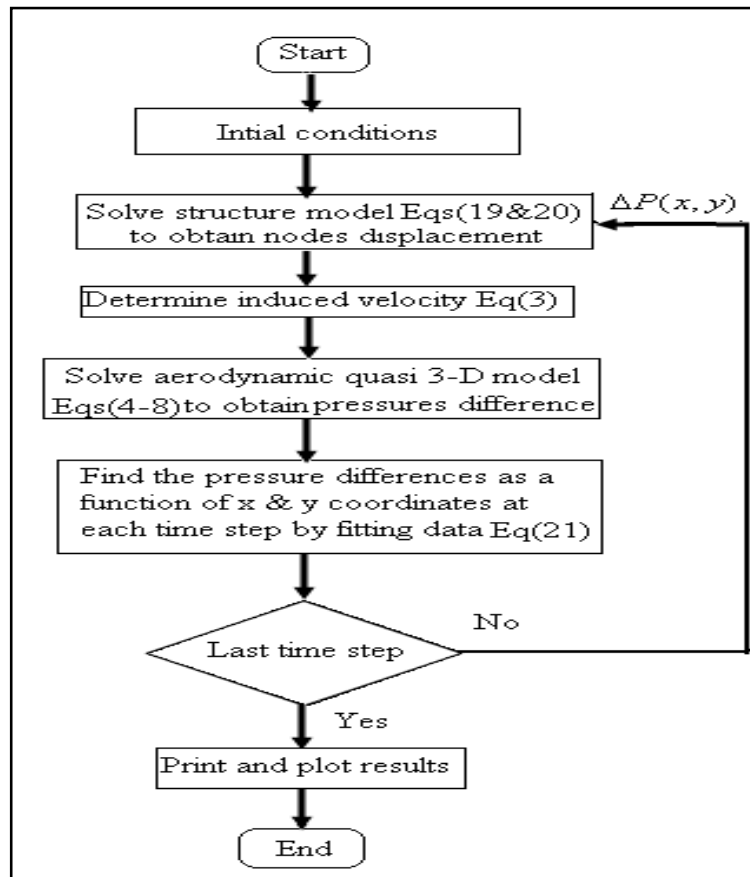


Figure (1) Wing-flap configuration and the coordinates system



Figure(2) Fully coupled fluid –structure

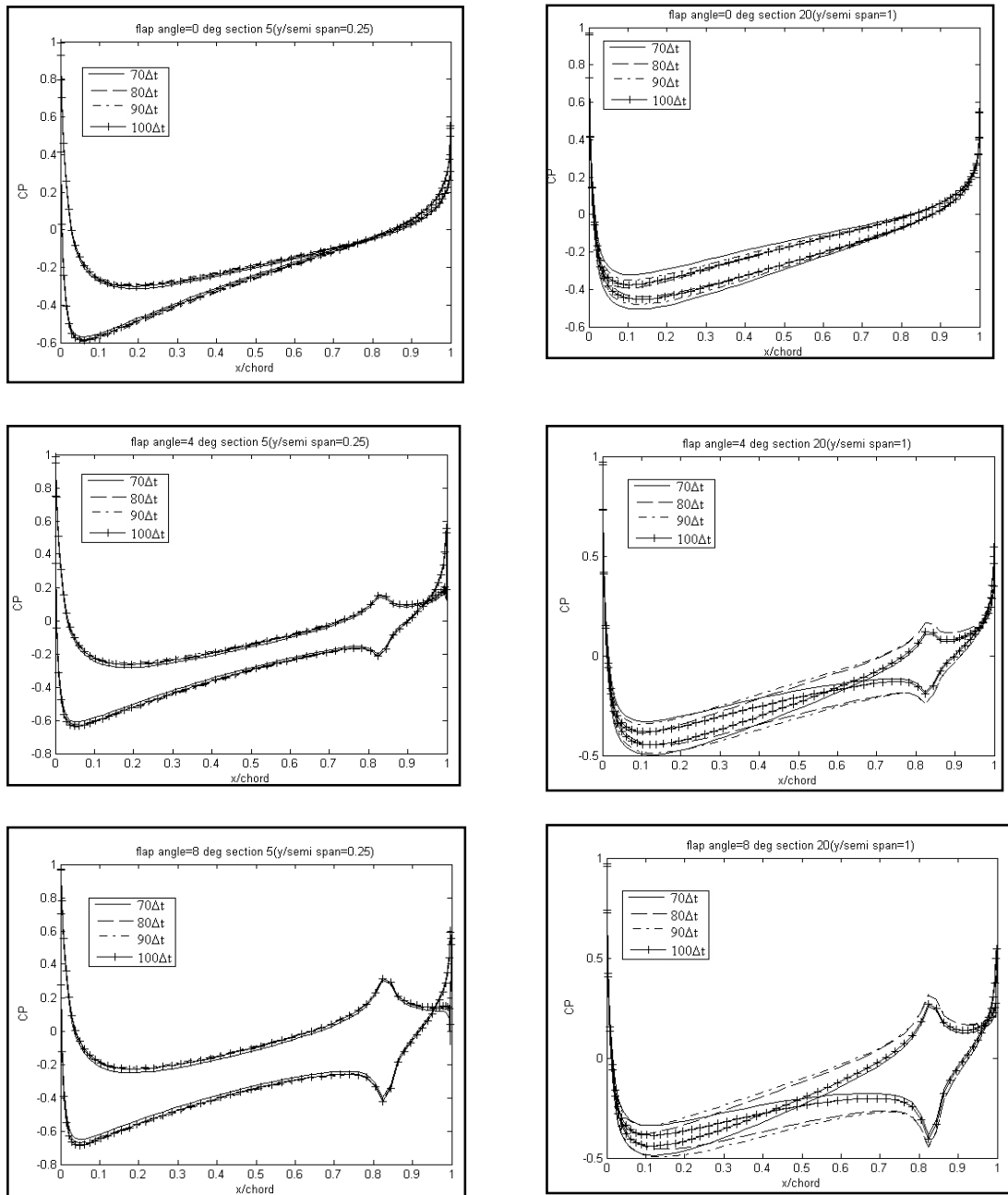


Figure (3) Effect of flap angle on the pressure distribution for rectangular wing –flap configuration ( $\alpha_g = 3$  deg. .NACA0012 section)

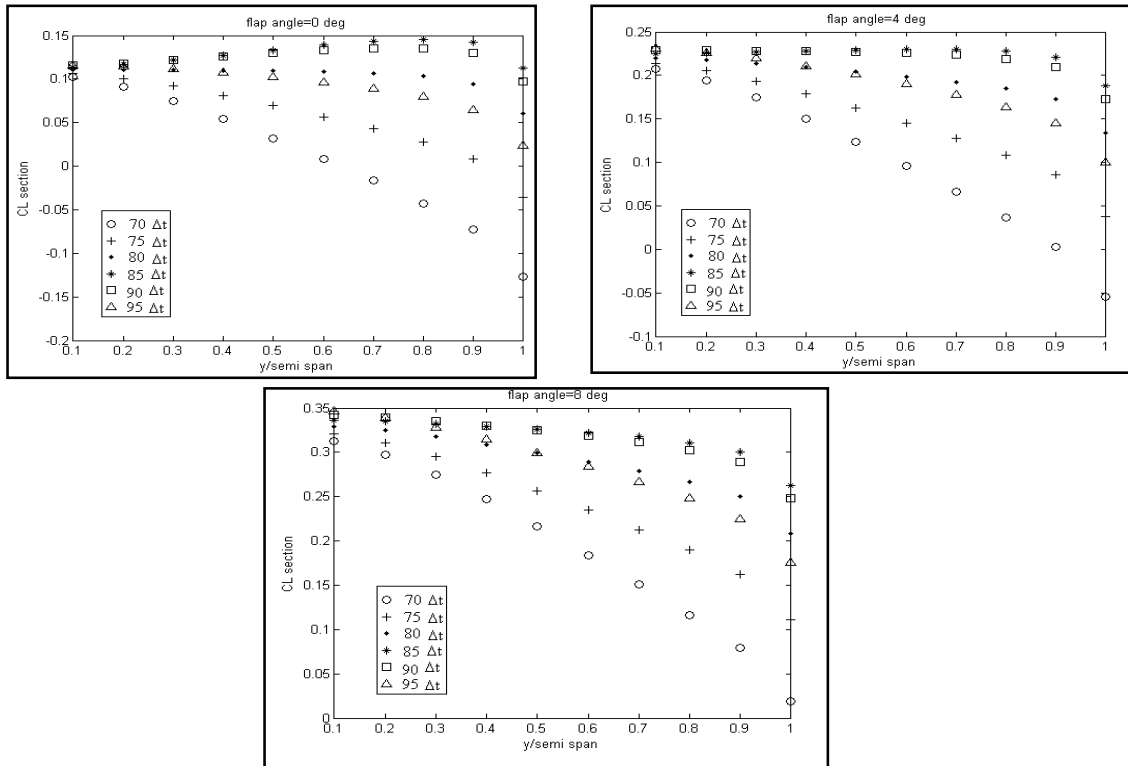


Figure (4) Effect of flap angle on lift coefficient along the semi span for rectangular wing –flap configuration ( $\alpha_g = 3 \text{ deg.}$  .NACA0012 section)

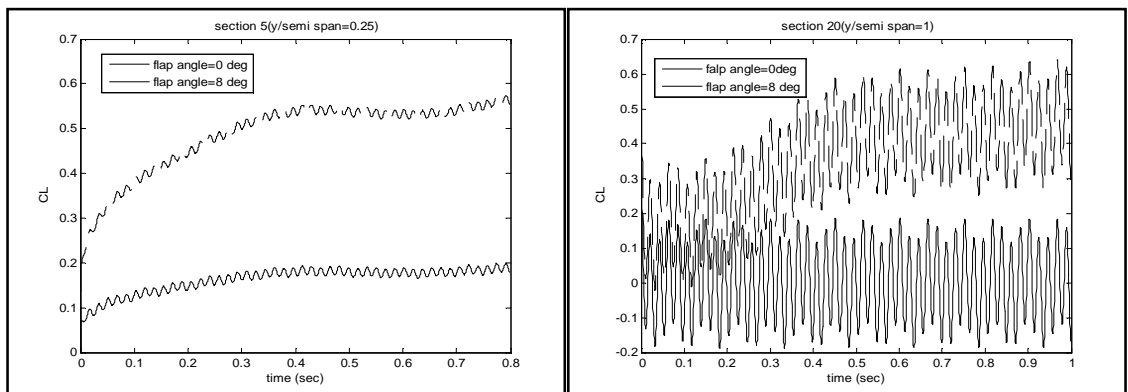


Figure (5) Time dependent behavior of lift coefficient at different flap angles for rectangular wing –flap configuration ( $\alpha_g = 3 \text{ deg.}$  .NACA0012 section)

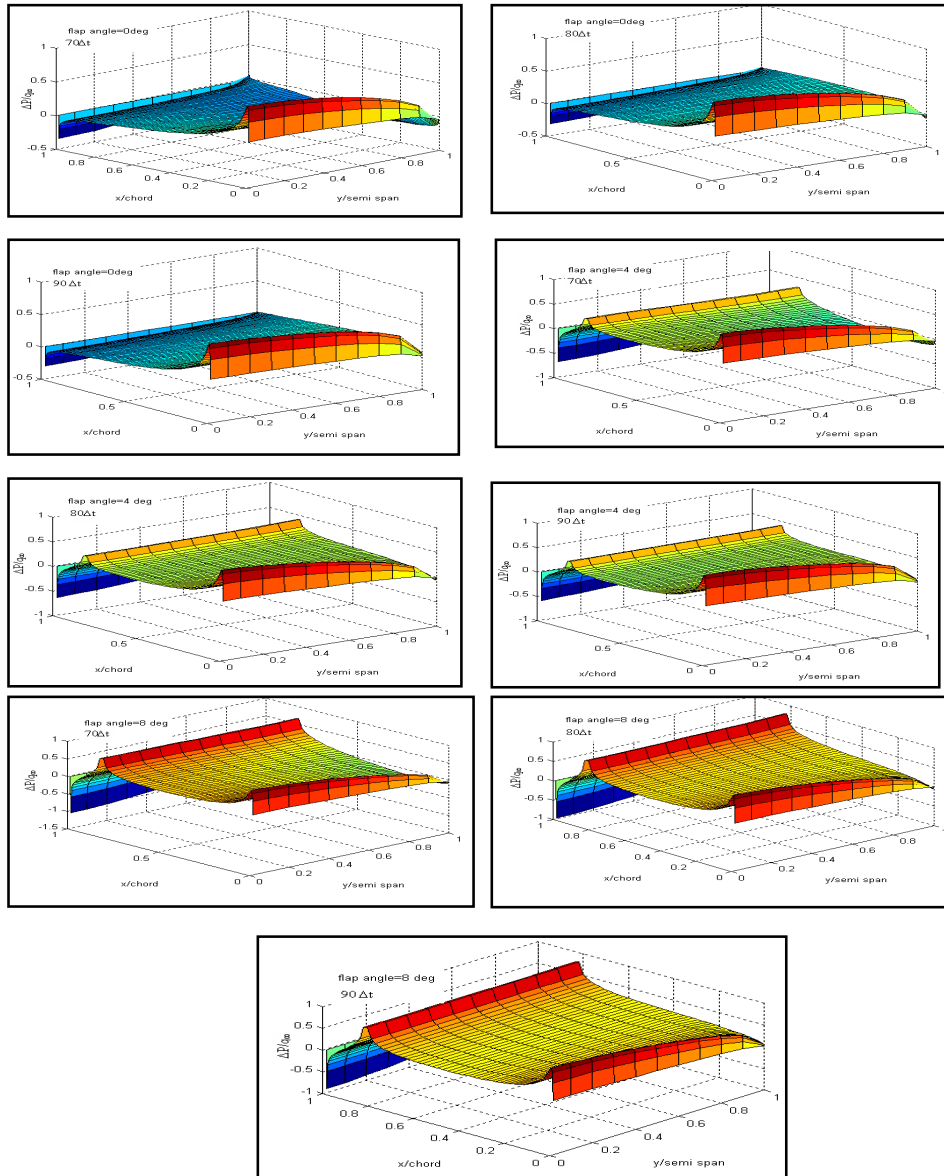


Figure (6) Effect of flap angle on the surface pressure difference at different times ( $\alpha_r = 3 \text{ deg.}$ ).

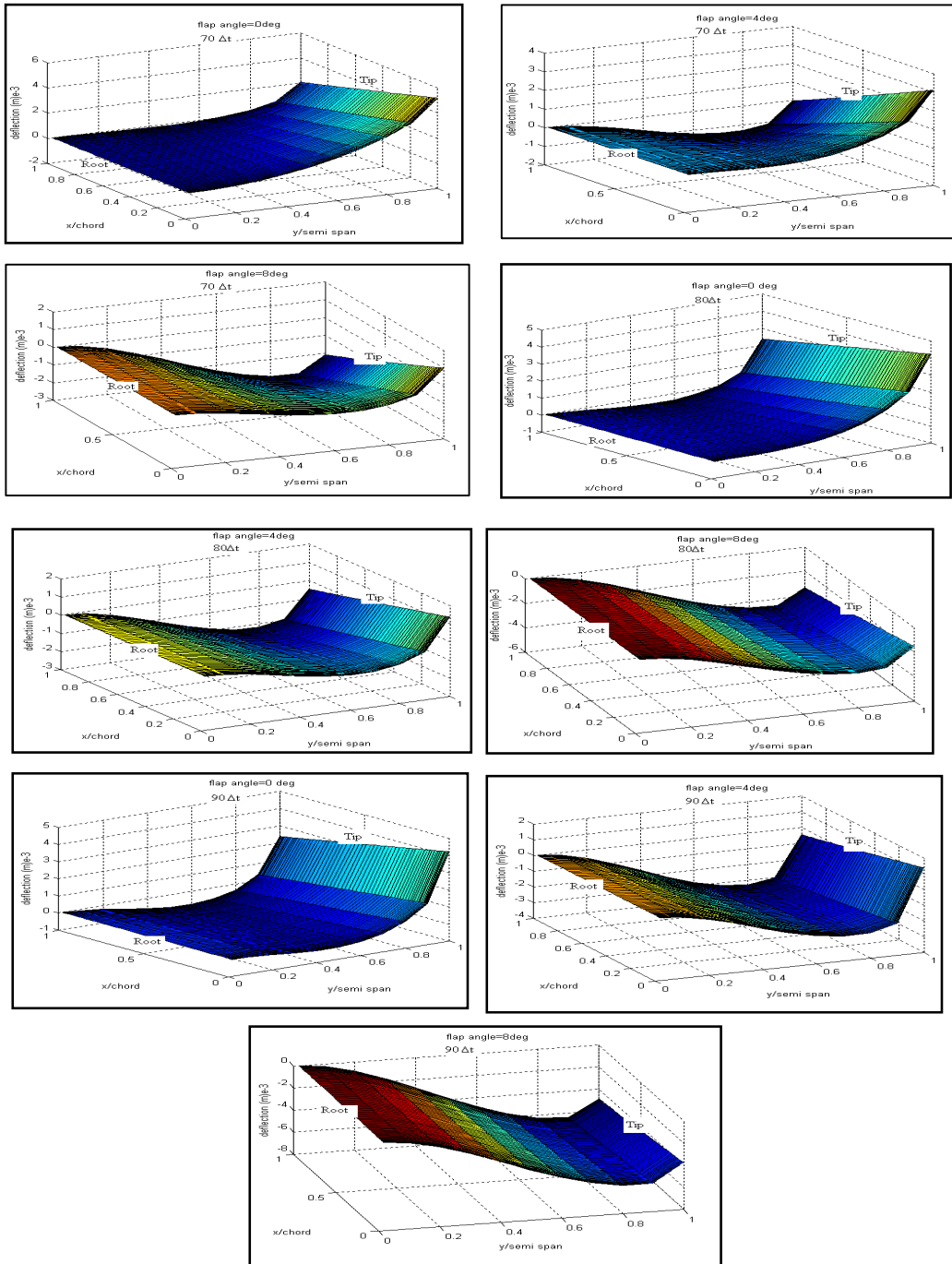


Figure (7) Effect of flap angle on the aeroelastic responses of the wing at different times ( $\alpha_g = 3 \text{ deg.}$ ).

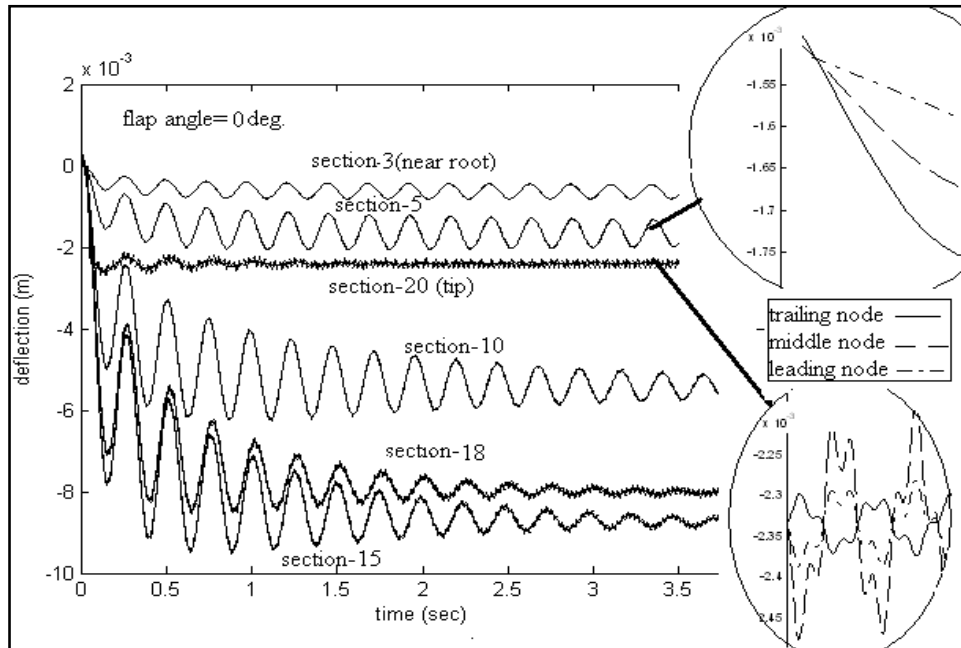


Figure (8-a) Time history of the wing deflection ( $\alpha_g = 3$  deg.)

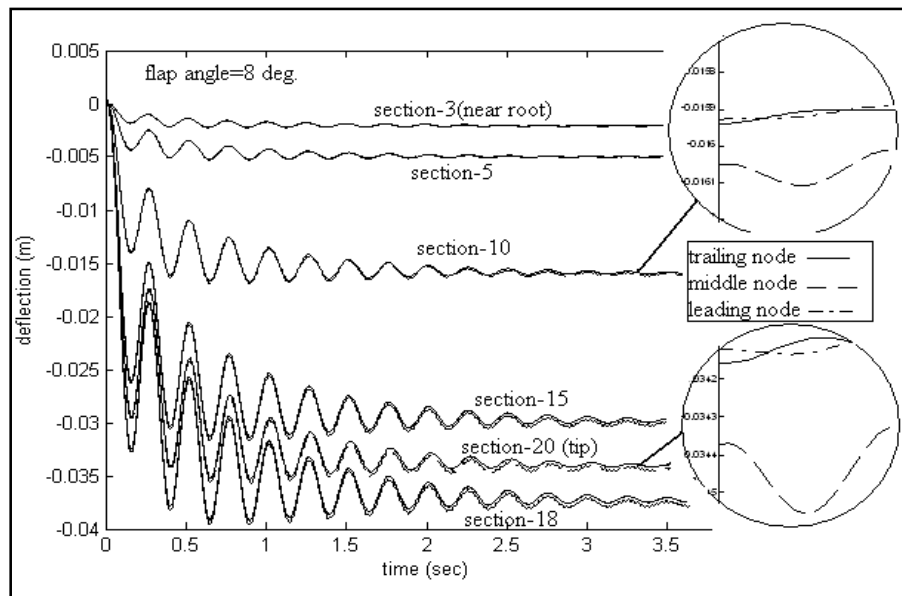


Figure (8-b) Time history of the wing deflection ( $\alpha_g = 3$  deg.)

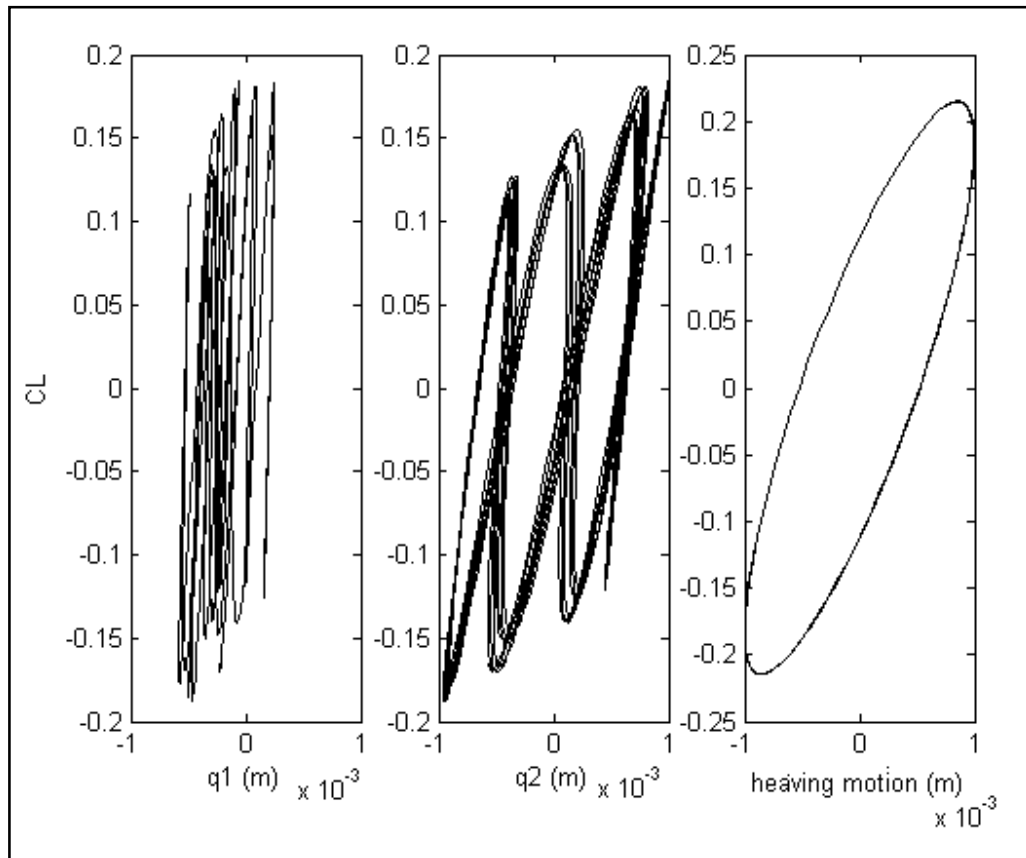


Figure (9) Unsteady lift coefficient vs. generalized coordinates  $q_1$  &  $q_2$  (present work) and airfoil harmonic motion [11].